Hindawi Publishing Corporation
Evidence-Based Complementary and Alternative Medicine
Volume 2014, Article ID 450592, 20 pages
http://dx.doi.org/10.1155/2014/450592

Research Article

In Silico Insight into Potent of Anthocyanin Regulation of FKBP52 to Prevent Alzheimer's Disease

Tzu-Chieh Hung,[1] Tung-Ti Chang,[2] Ming-Jen Fan,[3,4] Cheng-Chun Lee,[5] and Calvin Yu-Chian Chen[1,5]

[1] *Department of Biomedical Informatics, Asia University, Taichung 41354, Taiwan*
[2] *School of Chinese Medicine, College of Chinese Medicine, China Medical University, Taichung 40402, Taiwan*
[3] *Department of Biotechnology, Asia University, Taichung 41354, Taiwan*
[4] *Department of Biological Science and Technology, China Medical University, Taichung 40402, Taiwan*
[5] *School of Medicine, College of Medicine, China Medical University, Taichung 40402, Taiwan*

Correspondence should be addressed to Ming-Jen Fan; mjfan@asia.edu.tw and Calvin Yu-Chian Chen; ycc929@mit.edu

Received 21 October 2013; Revised 3 January 2014; Accepted 3 January 2014; Published 12 May 2014

Academic Editor: Fuu-Jen Tsai

Copyright © 2014 Tzu-Chieh Hung et al. This is an open access article distributed under the Creative Commons Attribution License, which permits unrestricted use, distribution, and reproduction in any medium, provided the original work is properly cited.

Alzheimer's disease (AD) is caused by the hyperphosphorylation of Tau protein aggregation. FKBP52 (FK506 binding protein 52) has been found to inhibit Tau protein aggregation. This study found six different kinds of anthocyanins that have high binding potential. After analyzing the docking positions, hydrophobic interactions, and hydrogen bond interactions, several amino acids were identified that play important roles in protein and ligand interaction. The proteins' variation is described using eigenvectors and the distance between the amino acids during a molecular dynamics simulation (MD). This study investigates the three loops based around Glu85, Tyr113, and Lys121—all of which are important in inducing FKBP52 activation. By performing a molecular dynamic simulation process between unbound proteins and the protein complex with FK506, it was found that ligand targets that docked onto the FK1 domain will decrease the distance between Glu85/Tyr113 and Glu85/Lys121. The FKBP52 structure variation may induce FKBP52 activation and inhibit Tau protein aggregation. The results indicate that anthocyanins might change the conformation of FKBP52 during binding. In addition, the purple anthocyanins, such as cyanidin-3-glucoside and malvidin-3-glucoside, might be better than FK506 in regulating FKBP52 and treating Alzheimer's disease.

1. Introduction

Alzheimer's disease (AD) is an irreversible degenerative disease of the brain. As time passes, a patient's memory, language, intelligent judgment, and motor skills will gradually deteriorate. In 2010, about 36 million people had AD worldwide [1], and the medical expenses incurred totaled approximately $604 billion [2]. Huge medical expenses are associated with AD, and since AD almost always occurs in people over 65 years old, this disease becomes a great social burden in an aging society.

Drugs for Alzheimer's disease include cholinesterase inhibitors (such as Aricept (donepezil), Exelon (rivastigmine), and Reminyl (galantamine) [3]) and N-methyl D-aspartate (NMDA) antagonists Memantine (such as Witgen and Ebixa). These two categories [4–6] of drugs only slow down or ameliorate the symptoms but do not treat or prevent the disease [7]. Recent studies have found that the brains of AD patients appear to have protein aggregations that cause brain damage. Hyper-phosphorylated Tau protein aggregation is associated with AD and worsens the symptoms [8]. There are a lot of treatments based on gene, protein, enzyme, and pathway association with disease in recent years [9–14]. Thus, by expressing FKBP52, the aggregation of Tau protein could be inhibited [15], and such inhibition could form the basis for a treatment of Alzheimer's disease [16].

FKBP52 belongs to the FK506-binding protein family, which has a peptidyl prolyl isomerase (PPIase) functional domain. This domain will modify amino acids sites 231 and 255 of the Tau protein and make the Tau protein more readily phosphorylated [17]. An immunosuppressive drug containing FK506 could bind in this domain and inhibit

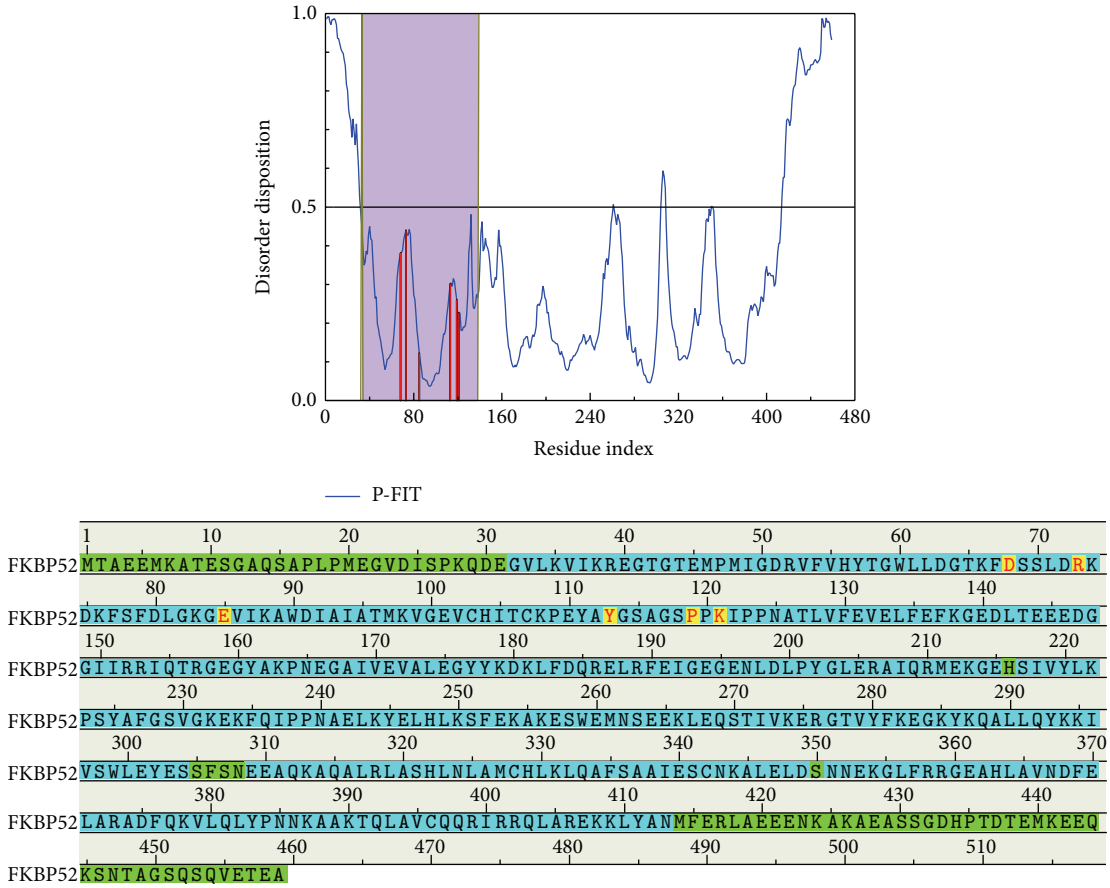

Figure 1: The disorder prediction and binding site detection. The blue curve in figure is the disorder disposition of each amino acid, the red lines indicate the residues of the important amino acids, and the purple region is the docking region, FK1 domain. The green regions of the amino-acid sequence show the predicted disordered regions, and the yellow regions, with the amino-acids noted in red mean important amino acids.

PPIase activity [18]. FKBP52 could bind with steroid receptors in FKBPs [19]. FKBP52 contains four domains: a FKBP12 domain 1 (FK1), a FKBP12 domain 2 (FK2), a C-terminal tetratricopeptide repeat domain (TPR), and a calmodulin binding domain. The FK1 domain has a proline-rich loop, which is the PPIase activity domain. Therefore, the FK1 domain is the immunosuppressant binding site of FKBP52. Although the sequence of the FK2 domain is similar to the sequence of FK1, this domain lacks PPIase activity and cannot interact with FK506. The TPR domain helps FKBP52 bind heat-shock protein 90 (HSP90) as a cochaperone to remove Tau. Finally, the calmodulin-binding domain can regulate the phosphorylation of the protein [18, 20, 21].

Several studies have demonstrated that since the FK1 domain can bind PPIase, PPIase cannot modify Tau protein. Consequently, the calcineurin function will decrease, and Tau protein phosphorylation will be inhibited [22–27]. Furthermore, FKBP52 will have a higher binding affinity for HSP90 and steroid receptors (which could act as a cochaperone [28, 29]) than FKBP51, which has a similar structure to FKBPs and can make microtubules more stable [20, 30]. Therefore, this cochaperone can bring about Tau protein degradation [31, 32]. The ligand binds the FK1 domain, activates FKBP52, and reduces Tau protein phosphorylation while removing abnormal Tau proteins, thus preventing AD [18].

Anthocyanidins are a family of vegetable flavonoids and are the primary components in producing plant color and are well-known water-soluble dyes. The six common kinds of anthocyanidin are pelargonidin (red-orange), peonidin (red), delphinidin, cyanidin, petunidin, and malvidin (different shades of purple) [33–35]. This study used delphinidin-3-glucoside (D3G), petunidin-3-glucoside (Pt3G), cyanidin-3-glucoside (C3G), malvidin-3-glucoside (M3G), peonidin-3-glucoside (P3G), and pelargonidin-3-glucoside (Pa3G) as test compounds. In recent years, it has been found that anthocyanins can regulate immunity [36], have anticancer [37–40] and anti-inflammatory properties [41], as well as having preventative functions in cardiovascular disease [42–44] and diabetes [45, 46]. In addition, they are antioxidants [47–51], have skin brightening properties [52–55], can aid erection [56], and contain many other health benefits. The current literature indicates that the antioxidant capacity of anthocyanins can prevent the deterioration of beta-amyloid protein type AD [57–60].

The Computer-Aided Drug Design (CADD) is an *in silico* simulation technique containing structure-based and

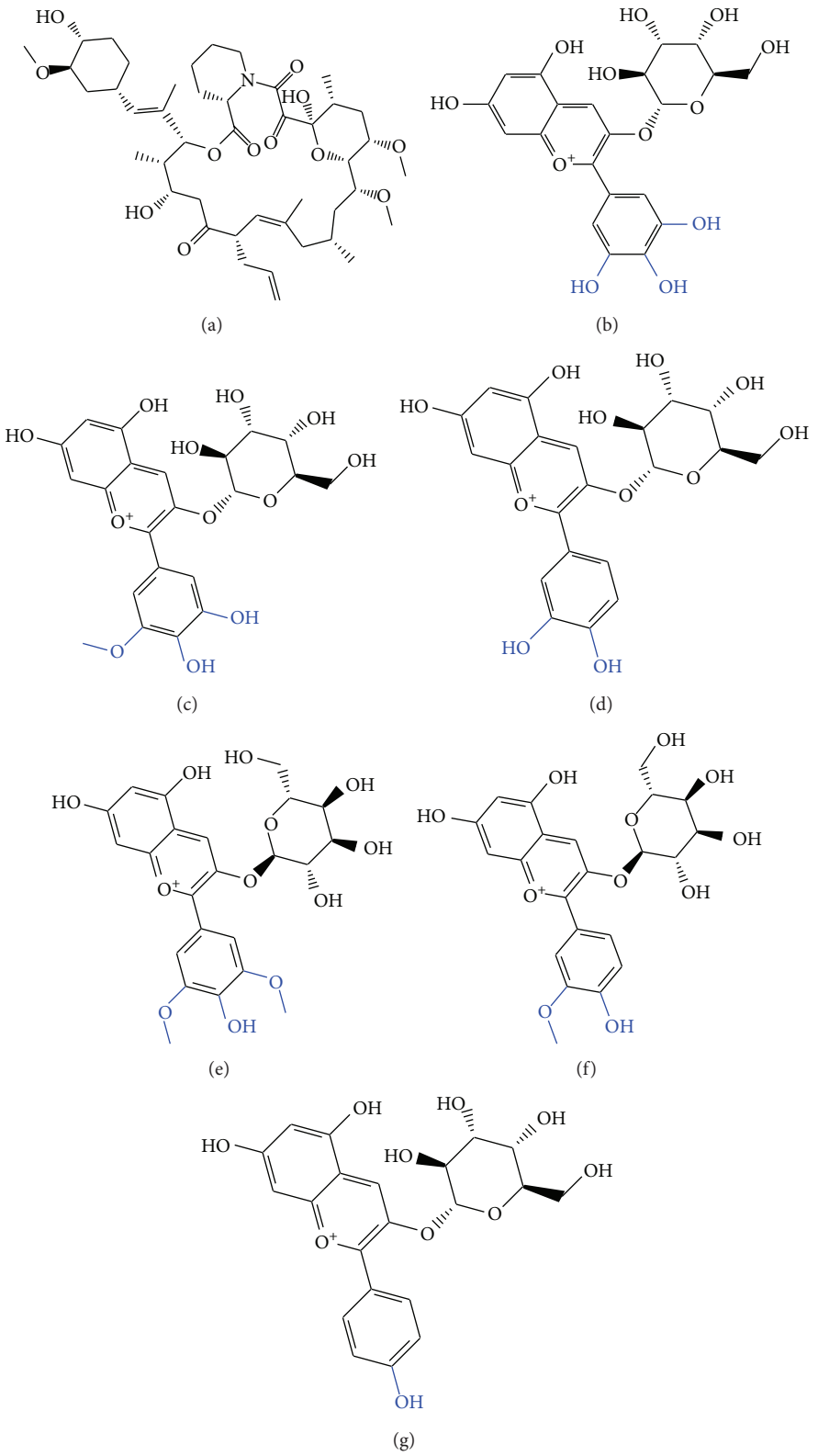

Figure 2: The structure of the ligand with (a) FK506 and (b) to (g) is D3G, Pt3G, C3G, M3G, P3G, and Pa3G, respectively, with the blue color indicating the differences.

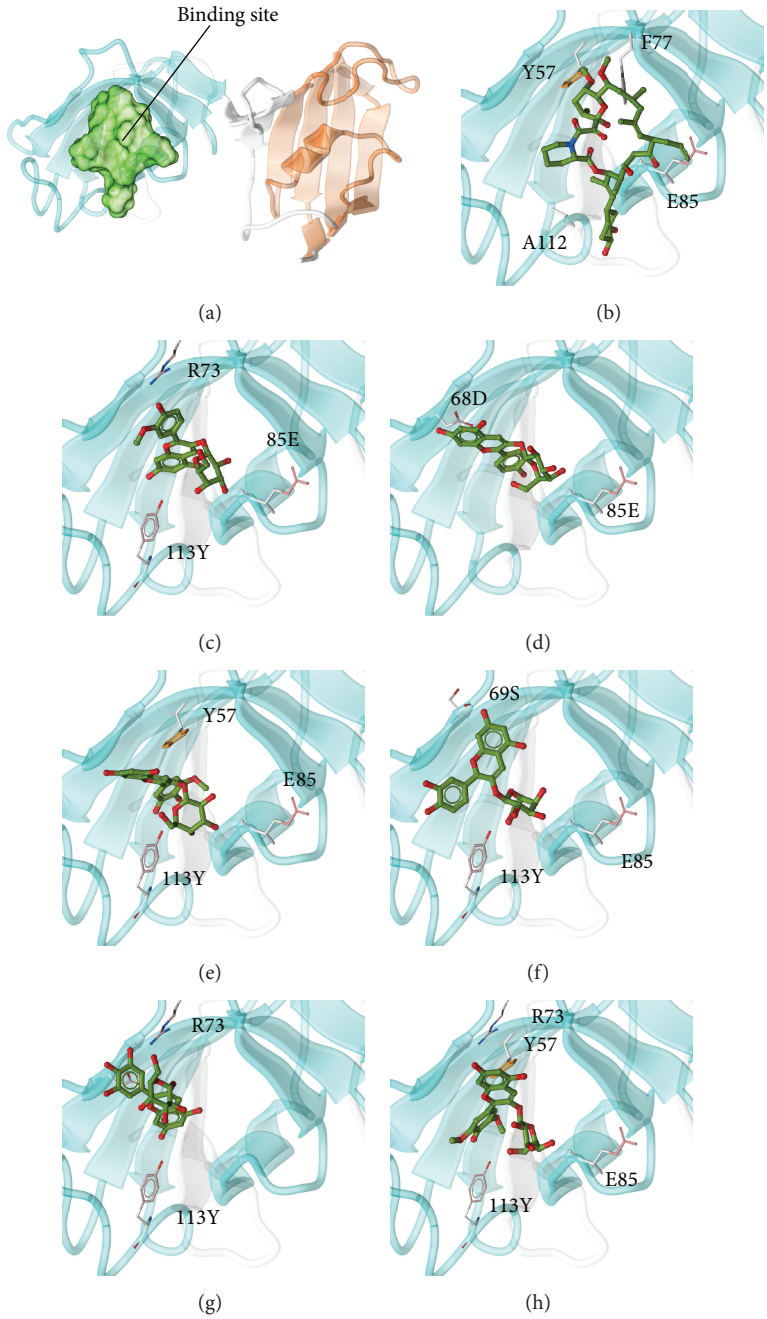

Figure 3: Docking poses of different ligands in the FKBP52 binding site. (a) Unbound protein, (b) FK506, (c) to (h) are D3G, Pt3G, C3G, M3G, P3G, and Pa3G, respectively.

ligand-based simulation. The main aspects of structure-based simulation are molecular docking, and molecular dynamics. The protein-ligand interactions could be analyzed by the above technique [61–63].

In this study FK506, an efficacy drug [27, 64–68] with associated side effects [69–73], is used as a control drug. Our purpose is to determine whether anthocyanins influence FKBP52 activation, leading to the reduction of hyper-phosphorylated Tau protein aggregations, and thereby relieving Alzheimer's disease. To analyze the effects of the different anthocyanins on FKBP52 activation, we will observe the transformation of the FKBP52 structure after binding and molecular dynamic simulation.

Recently report, the personalized medicine and biomedicine are necessary [74, 75] especially in rare diseases [76] and diagnosis [77]. The TCM is a famous personalized medicine. In order to compare the effect on FKBP52 with the anthocyanins and the compounds of Traditional Chinese Medicine (TCM), we screened the TCM Database@Taiwan (http://tcm.cmu.edu.tw/) for simultaneous docking. The TCM Database@Taiwan [78] contains 61,000 TCM compounds and is the largest TCM database in the world. Recently, TCM

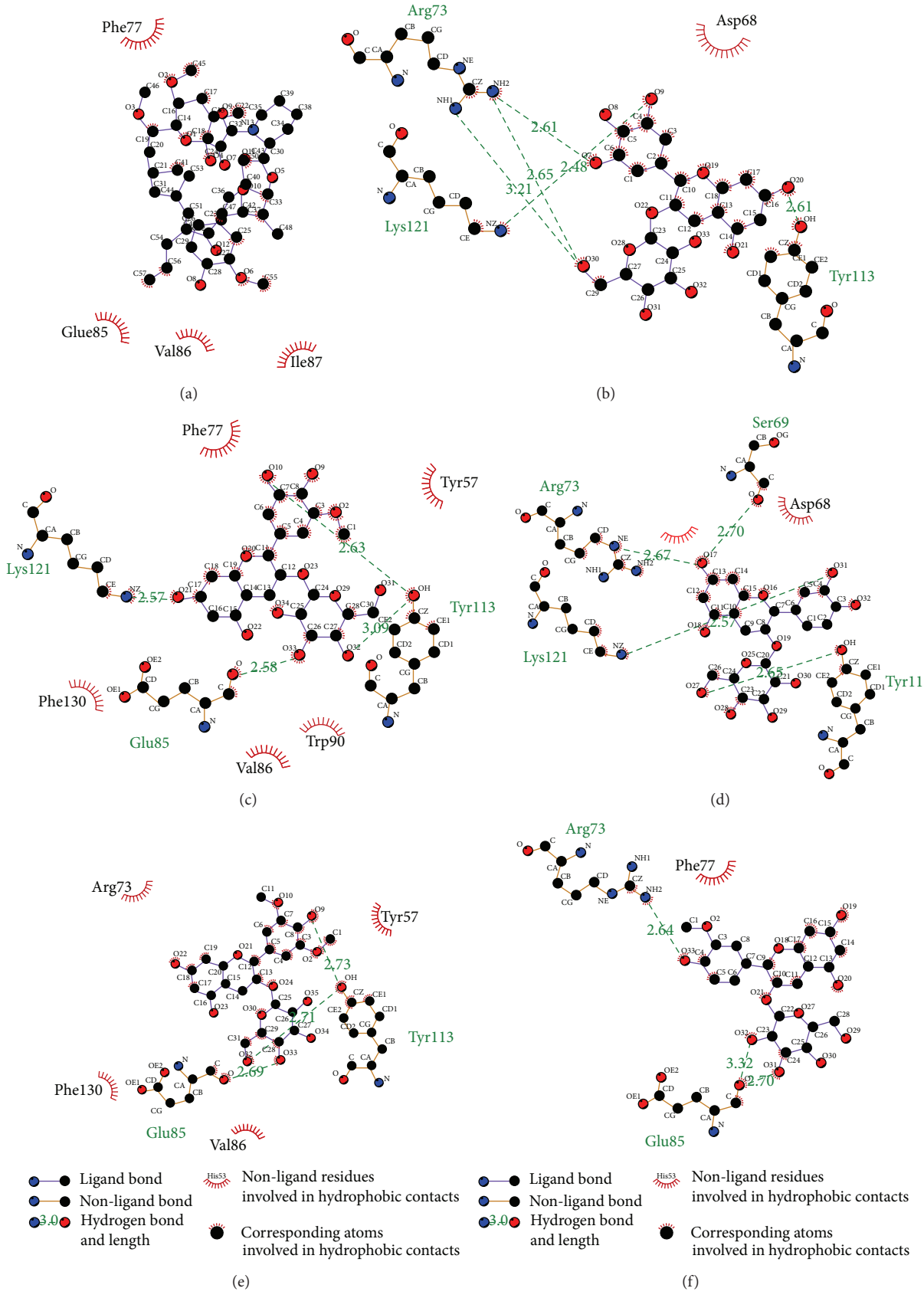

Figure 4: Continued.

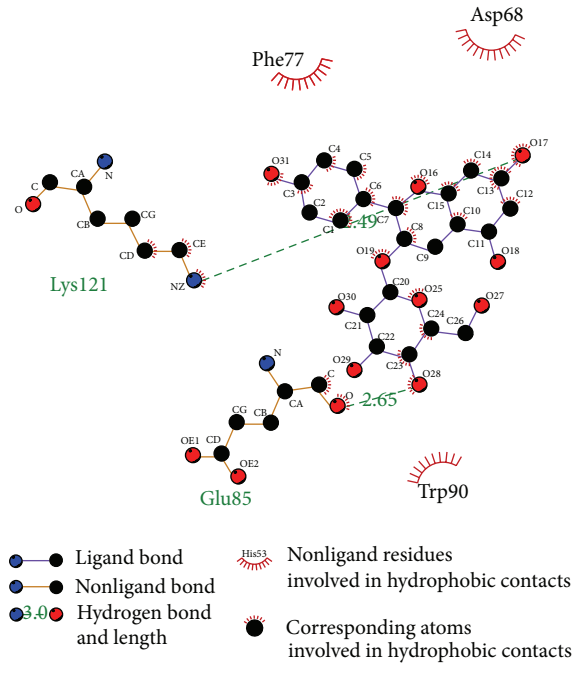

Figure 4: Ligplot illustrating protein-ligand interactions during docking. (a) FK506 and (b) to (g) indicate D3G, Pt3G, C3G, M3G, P3G, and Pa3G, respectively. Hydrophobic interactions are expressed by red spokes radiating towards the ligand atoms they contact in diagrams. Ligands are represented in purple. C, N, and O atoms are indicated in black, blue, and red, respectively.

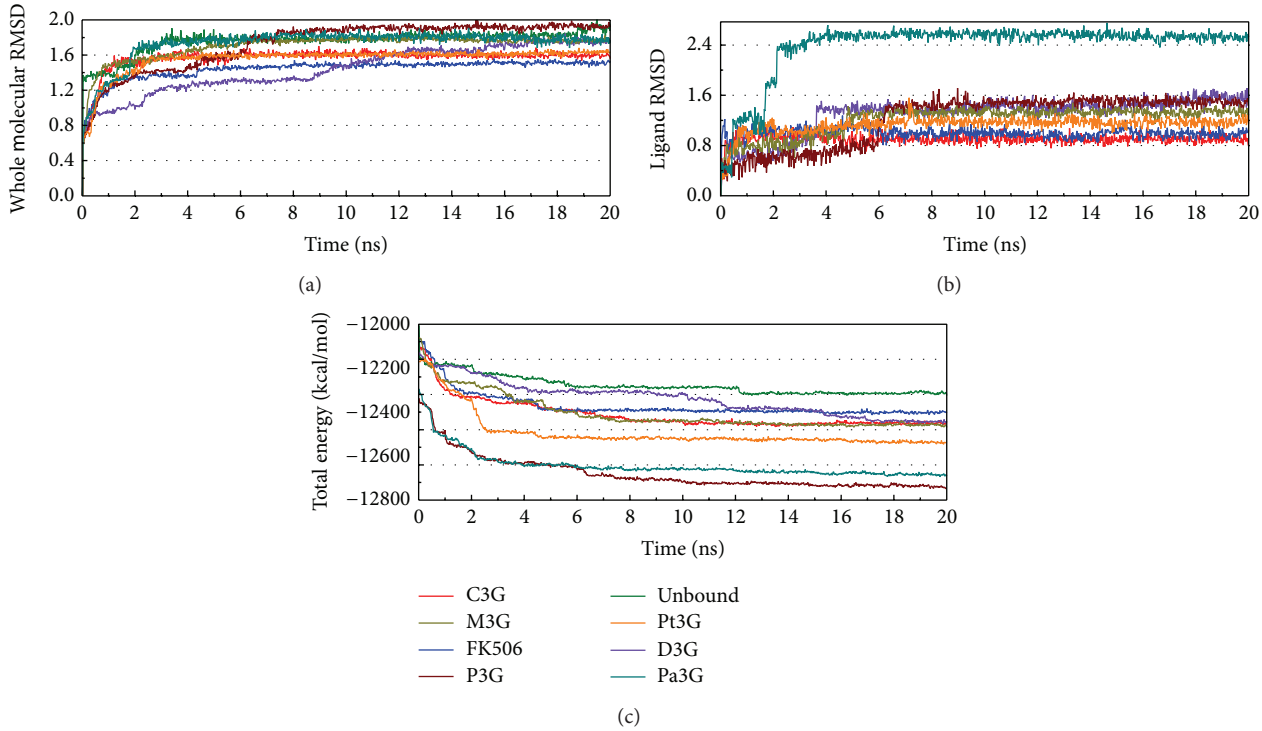

Figure 5: Measured trajectories during 20 ns MD. (a) Complex, (b) ligand, and (c) total energy during MD.

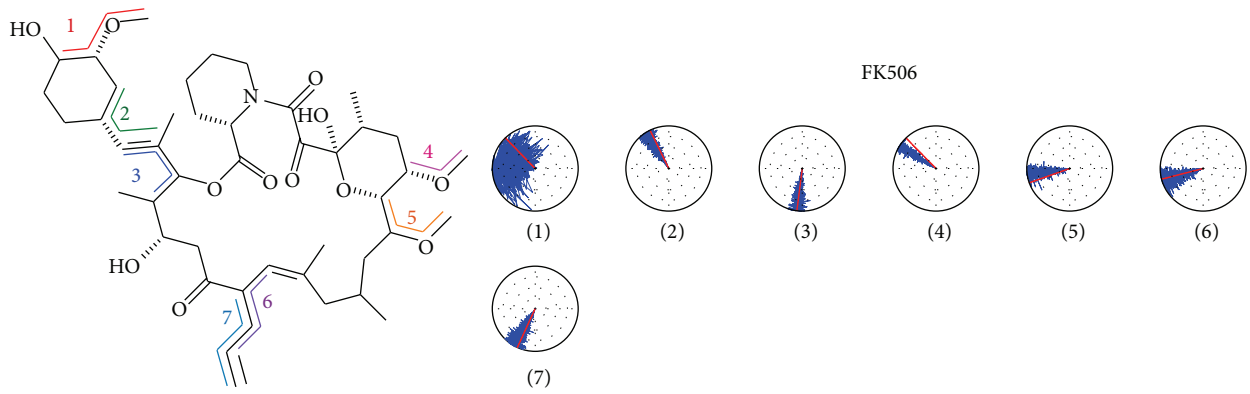

(a)

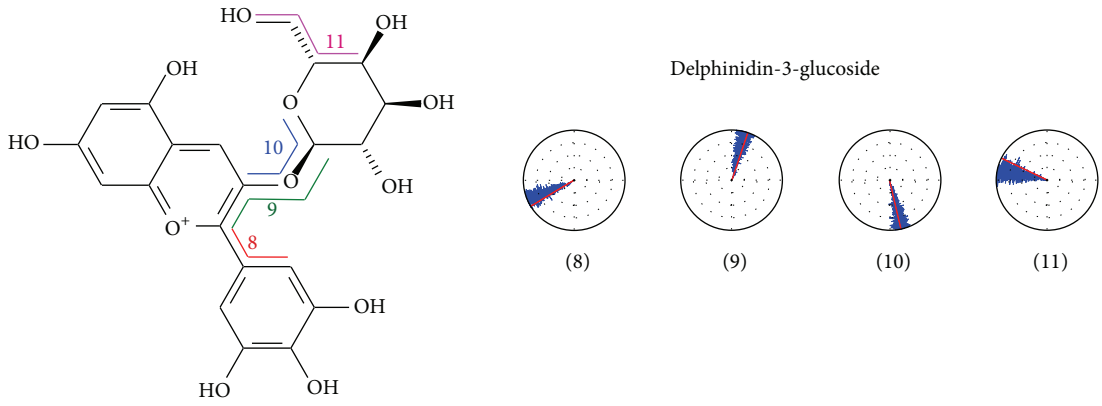

(b)

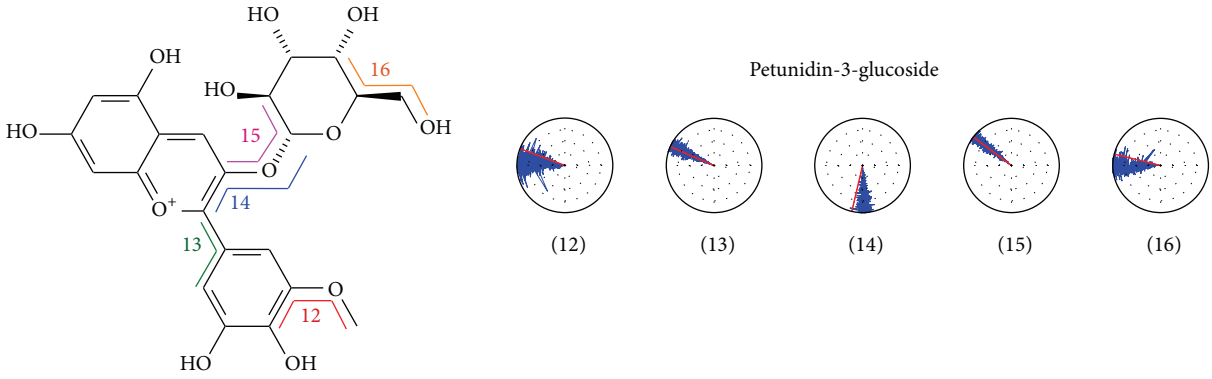

(c)

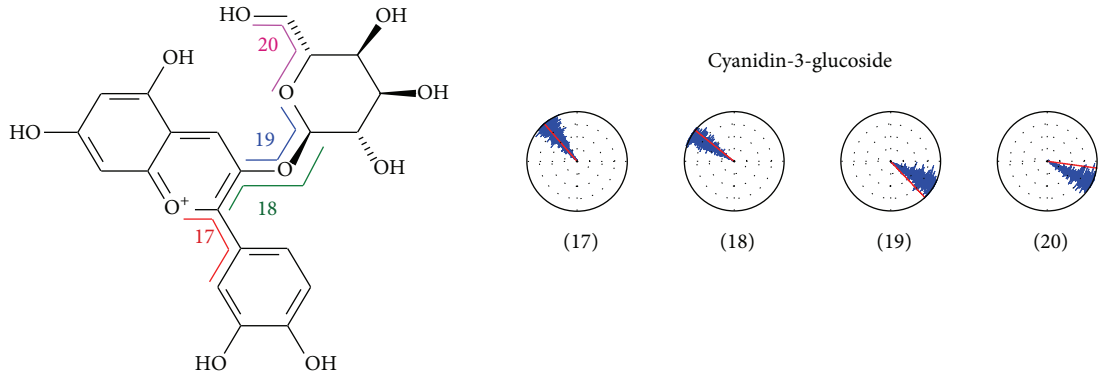

(d)

Figure 6: Continued.

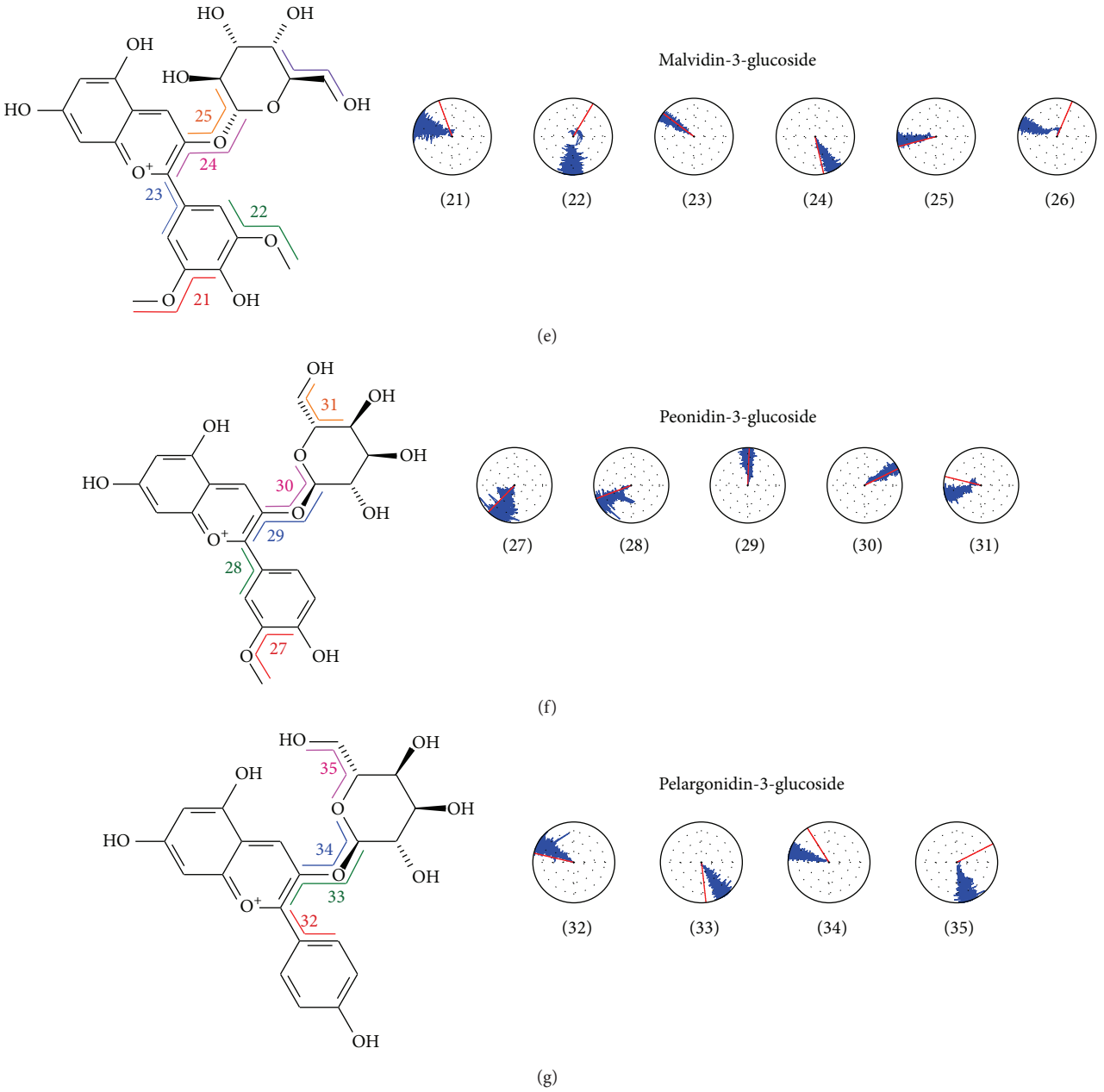

Figure 6: Torsion angles of anthocyanin during MD. Torsion angle measured is designated by the number which corresponds to the radar chart. The red and blue lines in the radar chart indicate the angle during time 0 and the period of MD.

database applied for stroke prevention [79], inflammation inhibition [80], pain regulation [81], cancer receptor inhibition [82, 83], and virus prevention [84, 85] by CADD and cloud-computing web server [86]. Thus, using CADD to analyze protein-ligand interaction is feasible in the research.

2. Materials and Methods

2.1. Data Collection. The FKBP52 protein structure was downloaded from the Protein Data Bank (PDB: 1Q1C) [87]. 1Q1C is the crystal structure of FKBP52 from amino acids 21 to 257. This structure includes the FK1 domain (amino acids 33 to 139) and the FK2 domain (amino acids 151 to 254). Current literature identifies the FK1 domain as the PPIase functional site and the FK506 binding site which is the FKBP52 activation site. Therefore, the FK1 domain is the binding site that detects the compounds of Traditional Chinese Medicine, by comparison with the control drug FK506. The six common anthocyanins are D3G, Pt3G, C3G, M3G, P3G, and Pa3G; their compounds and structures can be obtained from Pubchem [88].

2.2. Disorder Protein Detection. Disordered proteins are important in drug design, and thus protein structure and the

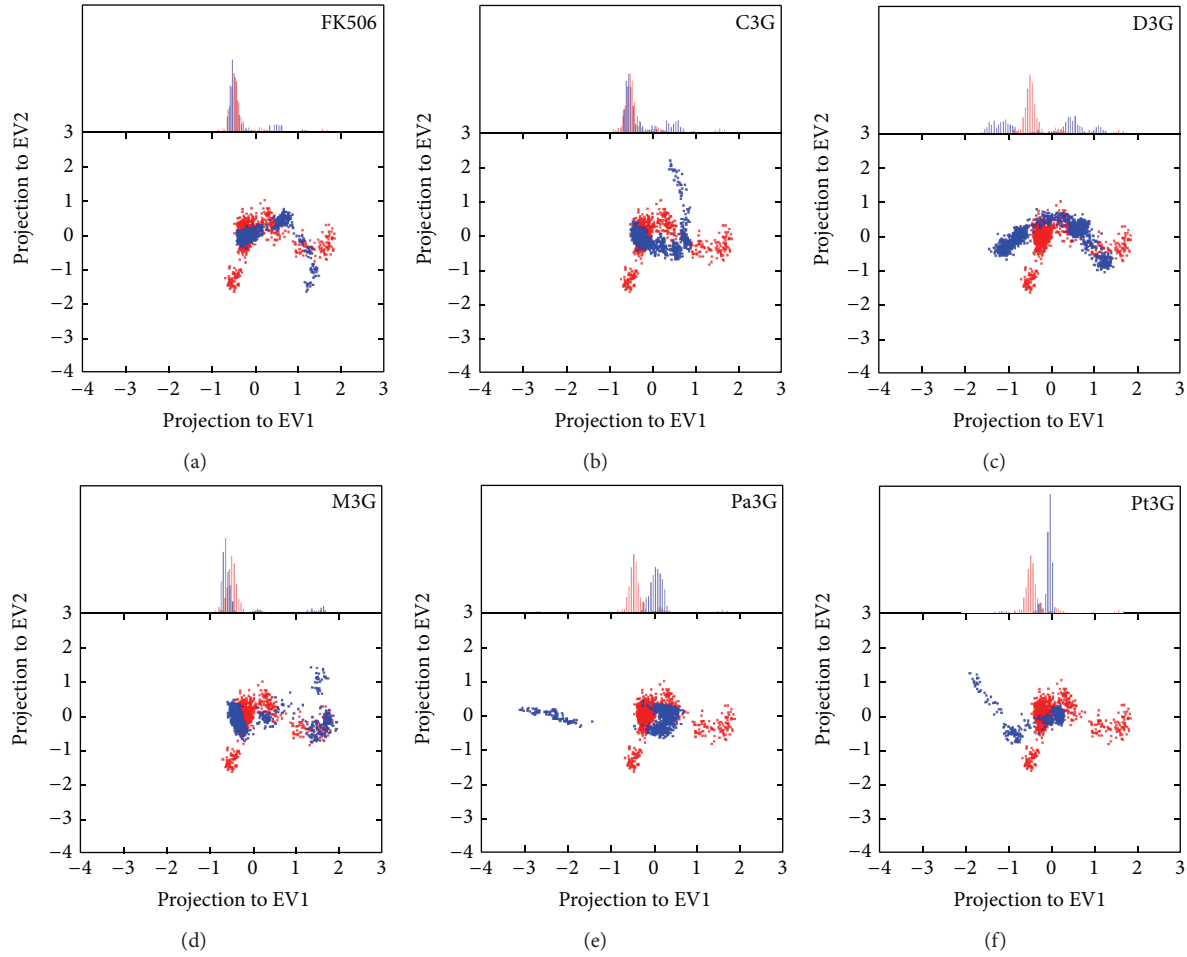

FIGURE 7: The PCA-eigenvector between ligand and unbound protein. The projection to the first two PCA-eigenvectors as X, Y axes based on the backbone of FKBP52 256 amino acids of MD is shown at the bottom of Figures 7(a) to 7(f). The red color indicates unbound protein and the blue is FKBP52 with ligand. The ligands in Figures 7(a) to 7(f) are FK506, C3G, D3G, M3G, Pa3G, and Pt3G.

ligand-interacting docking site should be detected [89, 90]. The protein sequence of CYP2C9 submitted to the Database of Protein Disorder (DisProt, http://www.disprot.org/) could predict the disordered region. Based on the result, the structure of docking site and drug efficiency could be discussed.

2.3. Docking. The control drug FK506 and anthocyanins (acting as ligands) were docked to the FK1 domain by LigandFit [91]. LigandFit, a program within Discovery Studio 2.5 (DS 2.5), is a receptor-rigid docking algorithm that uses a Monte Carlo simulation to measure the engaged position and orientation of the ligand when it targets the receptor of a crystal structure. The results were ranked based on docking score to assess the compatibility of the ligand and FKBP52 (1Q1C) crystal structure combination. If the ligand had a higher docking score than FK506, we could then use hydrophobic interaction analysis via Ligplot v.2.2.25 [92] to assess the interaction between ligand and protein amino acids.

2.4. Molecular Dynamics Simulation (MD). Molecular dynamics simulation (MD) is a Discovery Studio 2.5 program and the protocol used is CHARMM force field [93] with minimization, heating, equilibration, and production stages. The interval time of each step was 2 fs in the force field. The Minimize stage utilized steepest descent [94] and conjugate gradient [95] to run the maximum 500 steps in two minimizations. Besides Minimizing, other stages were analyzed using the SHAKE algorithm. The system was heated from 50 K to 310 K gradually in the 50 ps heating intervals and then subjected to the 200 ps Balance period. Finally, a 20-nanosecond production period was used as a canonical ensemble—meaning that in all systems, N, V (volume) and T (temperature) were the same.

After obtaining results from the molecular dynamic simulation, the root mean square deviation (RMSD) of the protein-ligand complex and the value of total energy were calculated using Discovery Studio 2.5. We also used Discovery Studio 2.5 to detect the presence of hydrogen bonds between the protein and ligand (based on 2.5 Å distance) and calculated the torsion of the ligand structure during the molecular dynamics simulation. The H-bond occupancy was recorded in a table. OriginPro 8.5 used the RMSD, the value of total energy, and the torsion of ligand structure to analyze and draw diagrams.

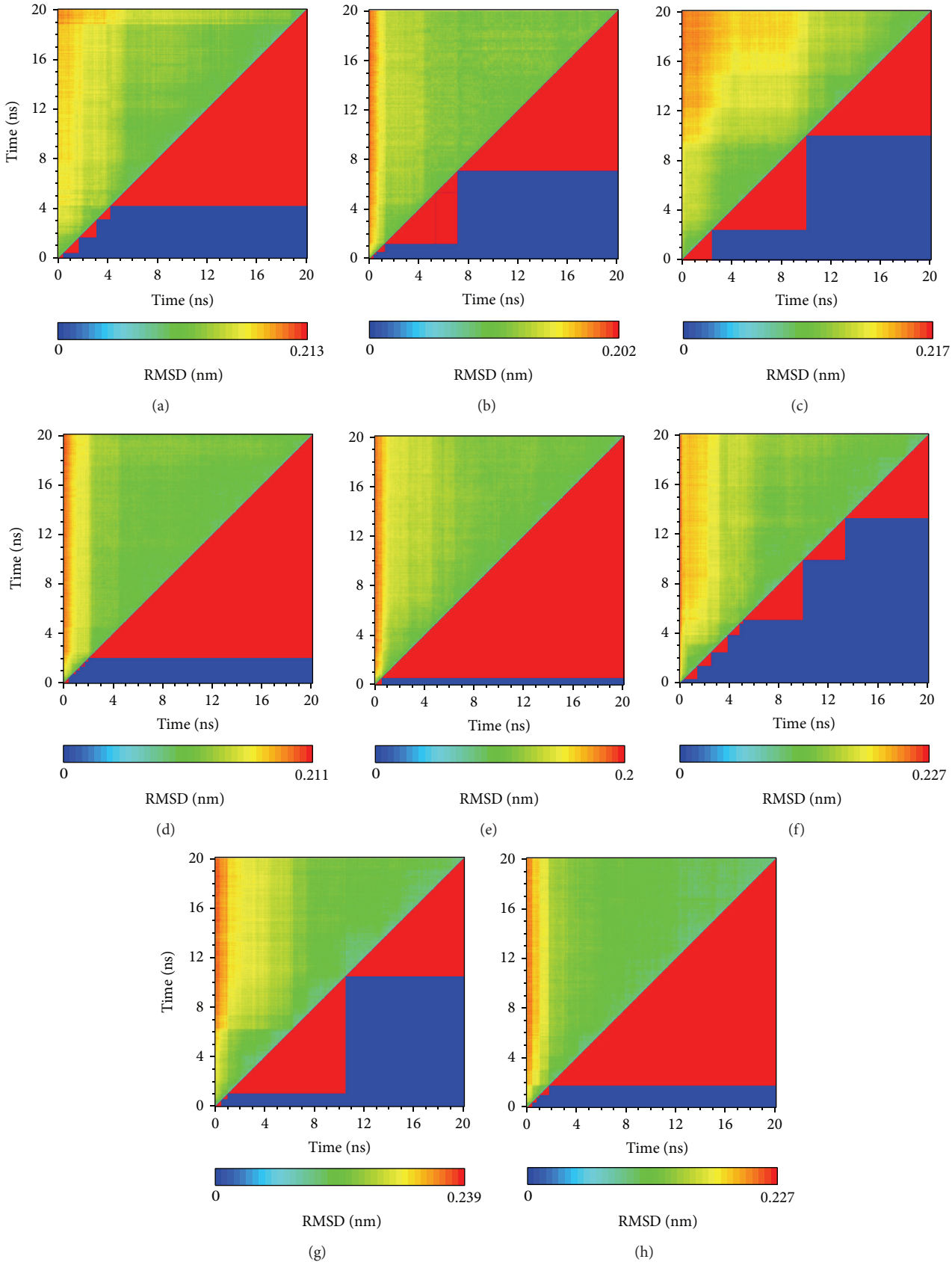

Figure 8: Clustering the ligand-protein interaction. (a) Unbound protein, (b) FK506, and (c) to (h) are D3G, Pt3G, C3G, M3G, P3G, and Pa3G, respectively. The mainly green triangle in upper left expresses the stability of the system, with the greater variation in red. The mainly red triangle in the lower right indicates groups calculated by RMSD variation during MD.

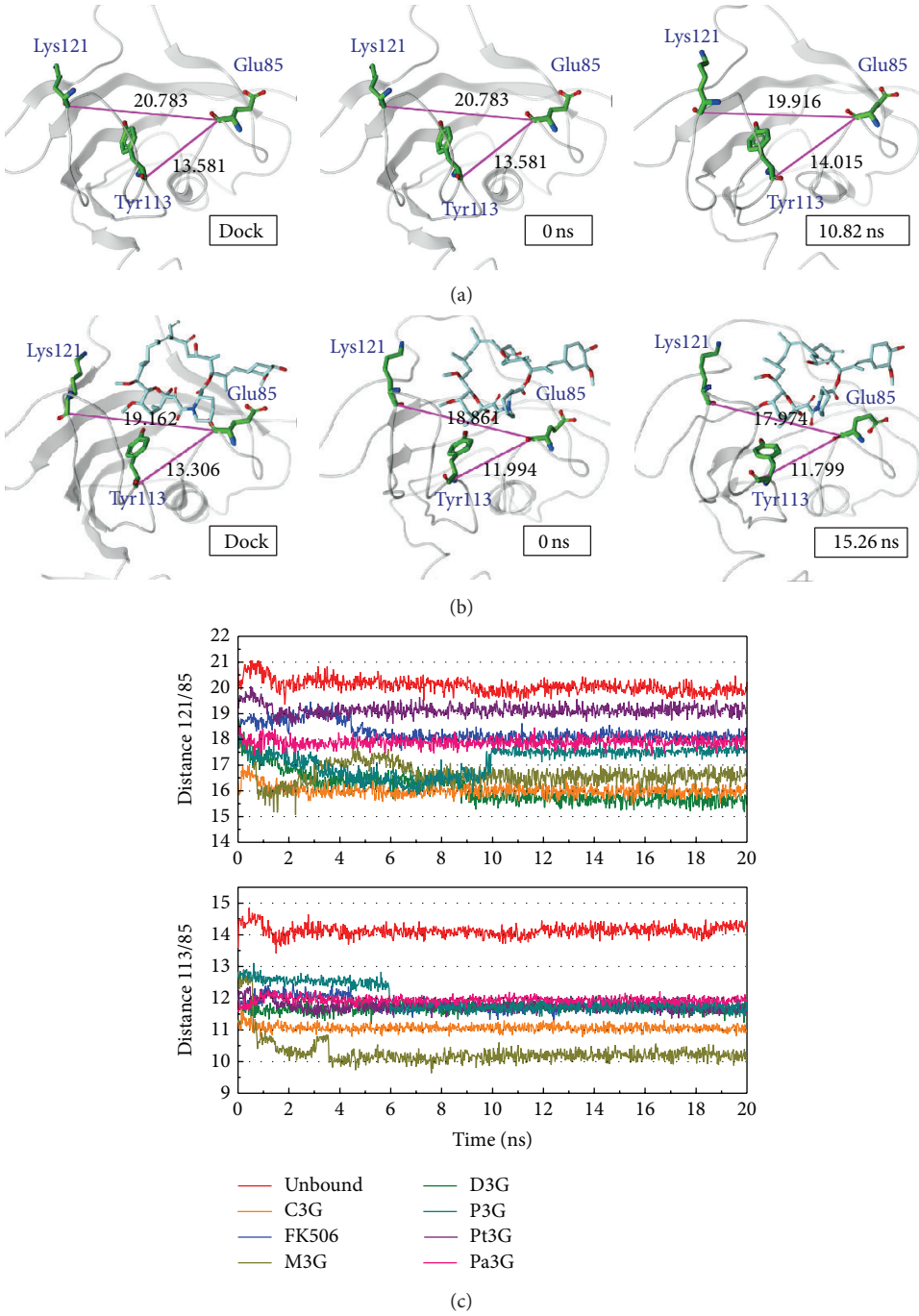

Figure 9: FKBP52 structure variation. (a) Unbound protein, (b) FK506, and (c) distance variation between unbound proteins with ligand.

The reference-identified eigenvector was used to represent the protein variation in protein interactions [96]. We calculated that the projection of the first two PCA (principal component analysis) eigenvectors would become the X and Y axes, based on the backbone of FKBP52's 256 amino acids of the MD data, to analyze the protein variation. The comparison between an unbound protein and a complex of protein with a ligand can describe the protein-ligand interaction.

Finally, we finished clustering based on the RMSD variation with a lapse of time in the molecular dynamic simulation and a threshold to distinguish the structure group of data. We identified the structure calculated in the intermediate period of the last population as the stable structure to determine that the interaction has been completed and balanced. The results of clustering can help analyze the variation of FKBP52 (1Q1C) structure under Docking, MD 0 ns and stability stages.

3. Results and Discussions

3.1. The Detection of Disorder Protein. The disordered protein is an unstructured protein. The docking site consists of a disorder protein that will make the complex stabilize difficultly.

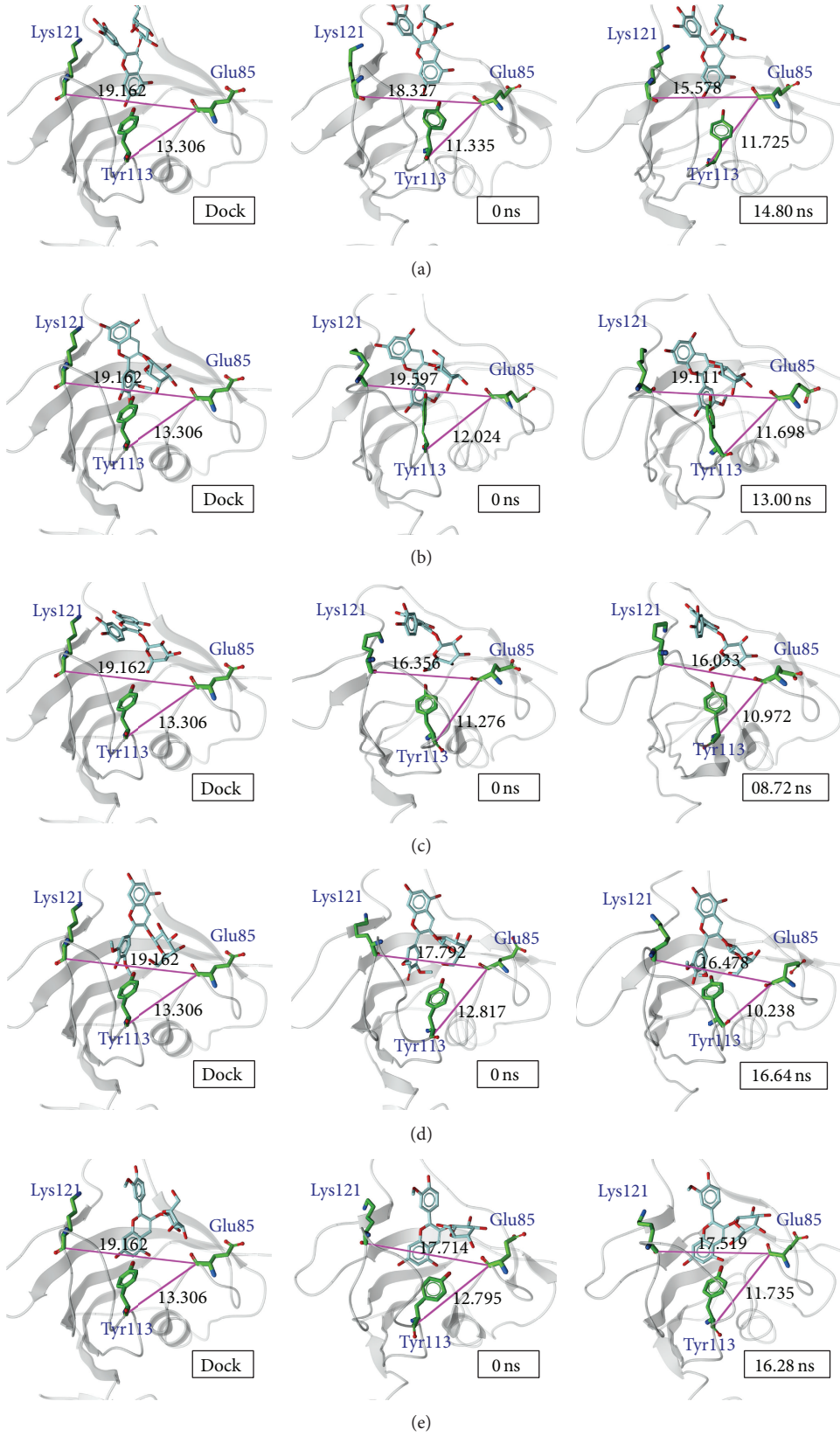

Figure 10: Continued.

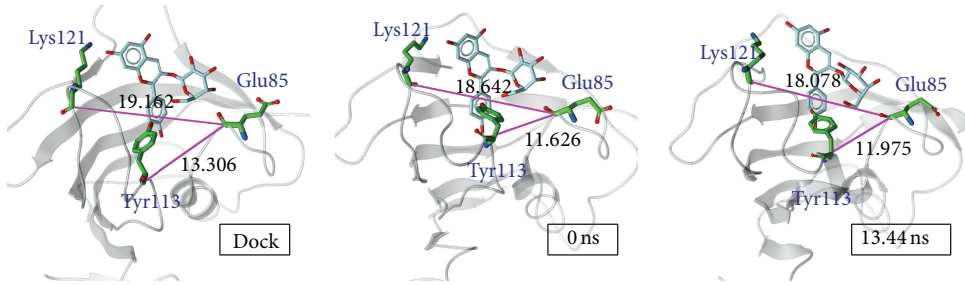

(f)

Figure 10: FKBP52 structure variation by anthocyanin target to FK1 domain. (a) D3G, (b) Pt3G, (c) C3G, (d) M3G, (e) P3G, and (f) Pa3G.

Table 1: Scoring functions of six anthocyanins and FK506 docking to FKBP52. The data is ranked by Dock Score.

Name	Dock Score	Binding Energy[#]	-PLP1	-PLP2
Delphinidin-3-glucoside	120.19	−199.264	31.6	44.69
Petunidin-3-glucoside	114.917	−160.598	62.24	71.86
Cyanidin-3-glucoside	112.451	−175.737	41.9	52.48
Malvidin-3-glucoside	111.318	−172.621	61.93	66.59
Peonidin-3-glucoside	105.531	−165.244	44.68	49.42
Pelargonidin-3-glucoside	94.527	−157.885	58.88	55.96
FK506[*]	**62.232**	**−202.882**	**58.04**	**50.16**

[*] Control.
[#] Unit: kcal/mol.

The disordered regions are defined as the disposition greater than 0.5 (Figure 1). The purple region in Figure 1 is FK1 domain which has been defined functional site of FKBP52. This result indicates that the docking site and important amino acids do not consist of disorder protein. Thus, the disorder protein effect on our result is weak and the complex can stabilize.

3.2. Molecular Docking. The results show the six common anthocyanins and control drug FK506 docking to FKBP52 (Table 1) ranked from top to bottom based on the docking score. The docking scores for anthocyanins were about 1.5 to 2 times greater than those for FK506. This indicates that these ligands had a greater binding force than FK506 for the FK1 domain. We selected the results of screening the TCM database@Taiwan based on PLP1 and PLP2 being better than anthocyanin, and then ranked the docking score (Table 2). There were nine compounds over the threshold, even bisindolylpyrrole CPB-53-594-5 was better than the control in all conditions. Although we have these candidates, anthocyanin can be easily assimilated in the diet and does not have side effects.

Six anthocyanins as the ligands were arranged by differences in structure without taking into consideration the Cis and Trans isoforms which are shown in blue in Figure 2. Although their main structures are similar, the different branches ensure that their general structures do not overlap in the docking process (Figure 3). This result indicates that the ligands are not similar in docking with the same general structure and that it is helpful to analyze the interaction with different anthocyanins docking to FKBP52.

Through ligplot v.2.2.25, Lys121, Tyr113, Glu85, and Arg73 were found to have a high percentage of H-bond and hydrophobic interactions (Figure 4), thus suggesting that they are important amino acids in FKBP52. The functional regions of FKBP52 [21, 87, 97–99] are identified as two loops containing Tyr113, Glu85, and Arg73 and are different between FK1 and FK2. This could determine whether PPIase functions or not, and the loop containing Lys121 will have an influence on calcineurin activity; therefore, these loops play an important role in ligand and protein interactions.

3.3. Molecular Dynamics

3.3.1. RMSDs and Total Energy Trajectories. The data generated from molecular dynamics was analyzed for protein-ligand RMSD, ligand RMSD, and total energy of ligands-FKBP52 and unbound FKBP52 (Figure 5). This result shows that the total energy of unbound FKBP52 is the highest, with the complex of protein with FK506 being second, and with anthocyanins being the lowest. A lower total energy implies a more stable protein-ligand complex; this result indicates that anthocyanins bound to FKBP52 are more stable than FK506 or unbound proteins. In Figure 5, based on the gentle curve of the RMSD and the total energy, the low variation of protein-ligand interaction can be seen. This result shows that the interactions had been completed in 20 ns and that the data is credible for analysis.

Table 2: Screening the TCM database docking to FKBP52 for results better than those for anthocyanin. The data are ranked by Dock Score.

Name	Herb	Dock Score	-PLP1	-PLP2
Saussureamine C	*Saussurea Iappa* CIarke	189.618	51.33	44.96
Chebulic acid	*PhyIIanthus urinaria* L	136.859	43.81	48.7
Bisindolylpyrrole-3[#]	*Lycogala epidendrum*	134.391	47.57	45.78
Nodifloridin A	*Lippia nodiflora* (L.) L. C. Rich.	133.342	45.56	55.25
Bisindolylpyrrole-5[#]	***Lycogala epidendrum***	**130.369**	**60.11**	**61.34**
Shogasulfonic acid A	*Celastrus paniculatus*	128.547	58.33	55.43
Tournefolic acid A	*Salvia miltiorrhiza*	124.716	45.92	50.98
Flazin	*Delphinium omeiense*	124.406	44.33	53.84
Phyllanthusiin E	*Melicope triphylla*	121.443	45.84	52.68
4-Gingesulfonic acid	*Celastrus paniculatus*	119.885	50.65	51.37
FK506[*]		**62.232**	**58.04**	**50.16**

[*] Control.
[#] The bisindolylpyrrole-3 is bisindolylpyrrole CPB-53-594-3, and bisindolylpyrrole-5 is bisindolylpyrrole CPB-53-594-5.

The torsion in MD demonstrates that the base structure will set appropriate positions quickly, and thus interactions to change FKBP52 will only occur by a slight twist and offset. Figure 6 presents the selected ligands that were found to be suitable in MD.

The H-bond plays an important role in protein and ligand interaction. We calculate the H-bond frequency of 1,000 interactions (0.02 ns is recorded as one interaction per 20 ns MD) while each ligand interacts with FKBP52 (Table 3). After analyzing the protein and ligand interactions from the docking process, the hydrophobic interactions, and the MD data, the results indicate that the amino acids Glu85, Tyr113, Lys121, Asp68, and Arg73 of FKBP52 formed many H-bonds during protein and ligand interaction (Table 4). After calculating the H-bond occupation of 7,000 interactions recorded from the seven ligands (FK506 and six anthocyanins), the amino acids with the three highest times of H-bond occupation were Glu85 (3099 times), Tyr113 (2357 times), and Lys121 (2135 times) in FKBP52. These occupations are obviously higher than the top four Asp68 (1794 times), top 5 Arg73 (1422 times), and others. It is suggested that Glu85, Tyr113, and Lys121 are important in FKBP52.

According to the PCA-eigenvector of the FKBP52 backbone atoms of residues 21–257 (Figure 7) and the different distributions of the first eigenvector between control (blue) and unbound protein (red), FK506 is described as a ligand and made the first eigenvector distribution move left compared to unbound proteins, but their distributions are still similar. The results of C3G and M3G are similar to FK506. The direction of Pa3G and Pt3G first eigenvector distribution is from minus to plus and this direction is different from other ligands (which go from plus to minus). This shows that C3G and M3G may cause FKBP52 structural variations to be the same as FK506 when the protein and ligand interact. On the other hand, Pa3G and Pt3G may have different effects on FKBP52, especially out-lying data from the first eigenvector of 0–5 ns in MD.

After protein and ligand interactions were finished, suitable protein structures were determined at 20 ns MD based on the curve of RMSD and the flattening of the total energy variation. After clustering, the data generated from MD in the same group indicate that their RMSD variation and structure are similar. The data generated from the calculations of the median of the last group period could be identified as stable structures (Figure 8). The results of clustering displaying C3G as ligand have the lowest RMSD variation and form the smallest group (only two groups) among unbound FKBP52 and seven ligands. One group of C3G and FKBP52 interaction in MD occurs in only the first twenty-eight out of 1000 data points, the others consist of the second group. This result indicates that if C3G performs as a ligand, FKBP52 will become stable in 0.58 ns and maintain the stability of the structure. Taking an analysis of clustering, the structures become stable in order of speed: C3G > (unbound protein) > Pt3G > Pa3G > D3G > FK506 > P3G > M3G.

Different FKBP52 stable structures in the docking process, at zero ns in MD, are observed, and this variation could be a result of protein and ligand interactions. The divergence of FKBP52 protein structure during MD between unbound protein and FK506 as a ligand was found to contain four loops in the FK1 domain, with each of them containing Arg73, Glu85, Tyr113, and Lys121, which would change their position during the MD period.

The result of ligplot and H-bond analysis shows that Glu85, Tyr113, and Lys121 had a more functional effect than the other amino-acids of FKBP52. Some references identify the two loops containing Glu85 and Tyr113 as the difference between the FK1 and FK2 domains, which function in PPIase immunosuppressive drug binding [21, 87, 97–99]. The loop with Lys121 has an influence on calcineurin activity, and the amino P119L of this loop is different in the FK1 domain between FKBP52 and FKBP51 [98]. Accordingly, it is feasible to describe the functional structure of FKBP52 by the distance variation of the three loops with Glu85, Tyr113, and Lys121 during docking, MD 0 ns, and stable stages.

There were obvious variations in the amino centroid positions of Glu85, Tyr113, and Lys121. Variations were found in the distance between Glu85/Tyr113 and Glu85/Lys121 but not between Tyr113/Lys121 (<1 Å). It was found that the distance between Glu85/Tyr113 increased from 13.581 Å to

Table 3: H-bond occupancy for FKBP (1Q1C) with six kinds of anthocyanin and FK506 for a simulation time of 20 ns.

Name	H-bond interaction	Occupancy
FK506	Tyr113:HH/O9	3.70%
	Tyr57:HH/O1	61.30%
	Tyr57:HH/O2	0.30%
Delphinidin-3-glucoside	Asp72:OD1/H37	3.00%
	Asp68:OD1/H38	1.10%
	Asp68:OD2/H38	0.20%
	Glu85:O/H43	51.80%
	Arg73:HH12/O7	1.50%
	Arg73:HH21	2.30%
	Arg73:HH22/O7	99.40%
	Lys121:HZ/O9	28.20%
	Lys121:HZ2/O9	26.40%
	Lyd121:HZ3/O9	22.60%
Petunidin-3-glucoside	Asp68:OD1/H45	2.80%
	Phe67:O/H45	2.30%
	Glu85:O/H56	100.00%
	Arg73:HH21/O22	1.10%
	Lys121:HZ1/O21	35.00%
	Lys121:HZ2/O21	43.90%
	Lys121:HZ3/O21	46.30%
	Trp90:HE1/O9	92.60%
	Tyr113:HH/O29	1.90%
	Tyr113:HH /O32	98.00%
Cyanidin-3-glucoside	Ser69:O/H39	97.80%
	Tyr113:OH/H48	2.30%
	Glu85:O/H49	55.20%
	Pro120:O/H53	93.30%
	Arg73:HE/O17	0.10%
	Arg73:HH11/O17	16.40%
	Tyr113:HH/O27	0.40%
	Tyr57:HH/O27	2.40%
Malvidin-3-glucoside	Tyr113:OH/H41	0.60%
	Tyr113:OH/H58	5.50%
	Glu85:O/H58	0.10%
	Arg73:HH12/O22	0.30%
	Arg73:HH21/O22	7.40%
	Arg73:HH22/O22	0.10%
	Tyr113:HH/O10	4.30%
	Tyr113:HH/O32	1.10%
Peonidin-3-glucoside	Tyr113:OH/H44	59.3%
	Val86:O/H44	60.2%
	Tyr113:OH/H52	57.7%
	Val86:O/H52	4.1%
	Glu85:O/H53	95.8%
	Glu85:O/H54	2.3%
	Arg73:HH12/O2	0.30%
	Tyr113:HH/O29	0.30%
	Tyr57:HH/O18	0.10%
Pelargonidin-3-glucoside	Asp68:OD1/H39	89.40%
	Asp68:OD2/H39	85.90%
	Tyr113:OH/H48	0.10%
	Glu85:O/H49	4.40%
	Arg73:HH21/O17	0.50%
	Arg73:HH22/O17	13.10%
	Lys121:HZ1/O17	1.70%
	Lys121:HZ2 /O17	8.40%
	Lys121:HZ3/O17	1.00%
	Tyr113:HH/O27	0.50%
	Tyr57:HH/O19	0.10%

H-bond occupancy cutoff: 2.5 Å.

14.015 Å, while the distance between Glu85/Lys121 shortened from 20.783 Å to 19.916 Å in unbound protein during three designed stages (Figure 9(a)). But in the case of FK506 as a ligand, the distances between Glu85/Tyr113 and Glu85/Lys121 decreased from 13.306 Å to 11.799 Å and from 19.162 Å to 17.974 Å (Figure 9(b)). From the differences from the unbound protein and FK506 as a ligand in MD, it is suggested that the ligands docking to the PPIase functional site will shorten Glu85/Tyr113 and Glu85/Lys121 during the three designed stages (Figure 9(c)).

In Tables 5 and 6 we calculate these two distances from the docking, MD 0 ns, MD stable, and MD 20 ns. To compare the variation from 20 ns and stable protein structure of each condition (unbound, FK506, and anthocyanins), all the differences are less than the threshold. The above description presents the structure of the stable condition, with the 20 ns group being similar. The variations of Glu85/Tyr113 and Glu85/Lys121 are thought to dock to the PPIase functional site and activate FKBP52; these variations may provide a credible method of detection. We find the average variation of anthocyanin as a ligand shortened by about 2 Å. Glu85/Tyr113 and Glu85/Lys121 decreased from 13.306 Å to 11.391 Å and from 19.162 Å to 17.134 Å. These distances obviously shorten after anthocyanins dock to FK1, especially to D3G, C3G, and M3G. When D3G is a ligand, Glu85/Tyr113 and Glu85/Lys121 are −1.581 Å and −3.584 Å. The variation distances presented in the case of C3G are −2.334 Å and −3.129 Å and of M3G are −3.068 Å and −2.675 Å. The results of P3G and Pa3G were similar as FK506. Although Pt3G as a ligand had the smallest variation, the distances were still shorter than in the unbound protein (Figure 10). The above results illustrate that ligand docking to FK1 domain will affect Glu85/Tyr113 and Glu85/Lys121 explicitly, and anthocyanin could target PPIase functional site to activate FKBP52.

4. Conclusions

This research shows that the structure generated from the largest number of a final clustering group can become a stable condition for the final structure. The function of the PPIase inhibition and the FKBP52 activation can be suggested

Table 4: Summary of interaction type, location, and frequency of test ligands following docking and MD simulation.

	Interaction location/type/frequency*									
Ligand	Glu85	Tyr113	Lys121	Asp68	Arg73	Ser69	Pro120	Trp90	Val86	Tyr57
FK506 docking										
FK506 ligplot	Y								Y	
FK506 MD		H								HH
D3G docking		H	H		HH					
D3G ligplot		H	H	Y	H					
D3G MD	H		HHH	HH	HHH					
Pt3G docking	H	H	H							
Pt3G ligplot	H	H	H					Y	Y	Y
Pt3G MD	H	HH	HHH	H	H			H		
C3G docking		H	H		Hπ	H				
C3G ligplot		H	H	Y	H	H				
C3G MD	H	HH			HH	H	H			H
M3G docking	H	HH			H					π
M3G ligplot	H	H			Y				Y	Y
M3G MD	H	HHHH			HHH					
P3G docking	H	H			H					
P3G ligplot	H				H					
P3G MD	HH	HHH			H				HH	H
Pa3G docking	H		HH	H						
Pa3G ligplot	H		H	Y				Y		
Pa3G MD	H	HH	HHH	HH	HH					H

*Each letter denotes one interaction.
π: pi-interaction.
Y: Hydrophobic interaction.
H: H-bond.

Table 5: Comparing amino distance variation from Lys121 to Glu85 while the protein is in an unbound condition and targets the ligand during docking and MD.

	Docking	0 ns	Stable	20 ns
	121/85	121/85	121/85	121/85
Unbound	20.783	20.783 (0)	19.916 (−0.867)	20.215 (−0.568)
506	19.162	18.861 (−0.301)	17.974 (−1.188)	17.990 (−1.172)
D3G	19.162	18.327 (−0.835)	15.578 (−3.584)	15.450 (−3.712)
Pt3G	19.162	19.597 (0.435)	19.111 (−0.051)	19.033 (−0.129)
C3G	19.162	16.356 (−2.806)	16.033 (−3.129)	16.199 (−2.963)
M3G	19.162	17.792 (−1.37)	16.487 (−2.675)	16.567 (−2.595)
P3G	19.162	17.714 (−1.448)	17.519 (−1.643)	17.587 (−1.575)
Pa3G	19.162	18.642 (−0.52)	18.078 (−1.084)	18.102 (−1.060)
Anthocyanin average	19.162	18.071 (−1.091)	17.134 (−2.028)	17.156 (−2.006)

Table 6: Comparing amino-acid distance variation from Tyr113 to Glu85 while the protein is in an unbound condition and targets the ligand during docking and MD.

	Docking	0 ns	Stable	20 ns
	113/85	113/85	113/85	113/85
Unbound	13.581	13.581 (0)	14.015 (0.43)	14.398 (0.817)
506	13.306	11.994 (−1.312)	11.799 (−1.507)	11.690 (−1.616)
D3G	13.306	11.335 (−1.971)	11.725 (−1.581)	11.626 (−1.680)
Pt3G	13.306	12.024 (−1.282)	11.698 (−1.608)	11.522 (−1.784)
C3G	13.306	11.276 (−2.03)	10.972 (−2.334)	10.945 (−2.361)
M3G	13.306	12.817 (−0.489)	10.238 (−3.068)	10.041 (−3.265)
P3G	13.306	12.795 (−0.511)	11.735 (−1.571)	11.891 (−1.415)
Pa3G	13.306	11.626 (−1.68)	11.975 (−1.331)	11.897 (−1.409)
Anthocyanin average	13.306	11.979 (−1.327)	11.391 (−1.915)	11.320 (−1.986)

according to the variation of Glu85/Tyr113, and Glu85/Lys121 indicates the FKBP52 structural variation. Anthocyanins might regulate FKBP52 to prevent Alzheimer's disease based on the structure variation of FKBP52, especially the purple anthocyanins C3G and M3G. According to these results, these two anthocyanins could be predicted to have a better effect than the others. Due to their greater efficiency and fewer side effects, anthocyanins may become a more appropriate medicine than FK506.

Conflict of Interests

The authors declare that there is no conflict of interests regarding the publication of this paper.

Authors' Contribution

Tzu-Chieh Hung and Tung-Ti Chang contributed equally to this paper.

Acknowledgments

This research was supported by Grants from the National Science Council of Taiwan (NSC102-2313-B-468-001, NSC102-2325-B039-001, NSC102-2221-E-468-027-), Asia University (ASIA100-CMU-2, ASIA101-CMU-2, 102-ASIA-07), and China Medical University Hospital (DMR-103-058, DMR-103-001, DMR-103-096). This study is also supported in part by Taiwan Department of Health Clinical Trial and Research Center of Excellence (DOH102-TD-B-111-004) and Taiwan Department of Health Cancer Research Center of Excellence (MOHW103-TD-B-111-03). The authors are grateful to Weng Leong Tou, Kuan-Chung Chen, and Hung-Jin Huang for their help in this research, and to Christine Quan for the help in translation correction. Finally, our gratitude goes to Tim Williams, Asia University.

References

[1] Alzheimer's Disease International, World Alzheimer Report 2009, 2009, http://www.alz.co.uk/research/world-report.

[2] A. Wimo and M. Prince, World Alzheimer Report 2010: The Global Economic Impact of Dementia, 2010, http://www.alz.co.uk/research/world-report-2012.

[3] N. A. Clarke and P. T. Francis, "Cholinergic and glutamatergic drugs in Alzheimer's disease therapy," *Expert Review of Neurotherapeutics*, vol. 5, no. 5, pp. 671–682, 2005.

[4] T. Voisin and B. Vellas, "Diagnosis and treatment of patients with severe Alzheimer's disease," *Drugs and Aging*, vol. 26, no. 2, pp. 135–144, 2009.

[5] C. Babiloni, C. Del Percio, R. Bordet et al., "Effects of acetylcholinesterase inhibitors and memantine on resting-state electroencephalographic rhythms in Alzheimer's disease patients," *Clinical Neurophysiology: Official Journal of the International Federation of Clinical Neurophysiology*, vol. 124, no. 5, pp. 837–850, 2013.

[6] P. T. Francis, M. J. Ramírez, and M. K. Lai, "Neurochemical basis for symptomatic treatment of Alzheimer's disease," *Neuropharmacology*, vol. 59, no. 4-5, pp. 221–229, 2010.

[7] F. Mangialasche, A. Solomon, B. Winblad, P. Mecocci, and M. Kivipelto, "Alzheimer's disease: clinical trials and drug development," *The Lancet Neurology*, vol. 9, no. 7, pp. 702–716, 2010.

[8] C. Duyckaerts, B. Delatour, and M. Potier, "Classification and basic pathology of Alzheimer disease," *Acta Neuropathologica*, vol. 118, no. 1, pp. 5–36, 2009.

[9] D.-Y. Lin, F.-J. Tsai, C.-H. Tsai, and C.-Y. Huang, "Mechanisms governing the protective effect of 17β-estradiol and estrogen receptors against cardiomyocyte injury," *Biomedicine*, vol. 1, no. 1, pp. 21–28, 2011.

[10] C.-C. Lee, C.-H. Tsai, L. Wan et al., "Increased incidence of Parkinsonism among Chinese with β-glucosidase mutation in central Taiwan," *BioMedicine*, vol. 3, no. 2, pp. 92–94, 2013.

[11] C.-H. Wang, W.-D. Lin, D.-T. Bau et al., "Appearance of acanthosis nigricans may precede obesity: an involvement of the insulin/IGF receptor signaling pathway," *BioMedicine*, vol. 3, no. 2, pp. 82–87, 2013.

[12] Y.-M. Chang, B. K. Velmurugan, W.-W. Kuo et al., "Inhibitory effect of alpinate Oxyphyllae fructus extracts on Ang II-induced cardiac pathological remodeling-related pathways in H9c2 cardiomyoblast cells," *BioMedicine*, vol. 3, no. 4, pp. 148–152, 2013.

[13] I. C. Chou, W.-D. Lin, C.-H. Wang et al., "Association analysis between Tourette's syndrome and two dopamine genes (DAT1, DBH) in Taiwanese children," *BioMedicine*, vol. 3, no. 2, pp. 88–91, 2013.

[14] W.-Y. Lin, H.-P. Liu, J.-S. Chang et al., "Genetic variations within the PSORS1 region affect Kawasaki disease development and coronary artery aneurysm formation," *BioMedicine*, vol. 3, no. 2, pp. 73–81, 2013.

[15] B. Chambraud, E. Sardin, J. Giustiniani et al., "A role for FKBP52 in Tau protein function," *Proceedings of the National Academy of Sciences of the United States of America*, vol. 107, no. 6, pp. 2658–2663, 2010.

[16] J. Giustiniani, M. Sineus, E. Sardin et al., "Decrease of the immunophilin FKBP52 accumulation in human brains of alzheimer's disease and FTDP-17," *Journal of Alzheimer's Disease*, vol. 29, no. 2, pp. 471–483, 2012.

[17] J. Koren III, U. K. Jinwal, Z. Davey, J. Kiray, K. Arulselvam, and C. A. Dickey, "Bending tau into shape: the emerging role of peptidyl-prolyl isomerases in tauopathies," *Molecular Neurobiology*, vol. 44, no. 1, pp. 65–70, 2011.

[18] W. Cao and M. Konsolaki, "FKBP immunophilins and Alzheimer's disease: a chaperoned affair," *Journal of Biosciences*, vol. 36, no. 3, pp. 493–498, 2011.

[19] C. L. Storer, C. A. Dickey, M. D. Galigniana, T. Rein, and M. B. Cox, "FKBP51 and FKBP52 in signaling and disease," *Trends in Endocrinology and Metabolism*, vol. 22, no. 12, pp. 481–490, 2011.

[20] B. Chambraud, H. Belabes, V. Fontaine-Lenoir, A. Fellous, and E. E. Baulieu, "The immunophilin FKBP52 specifically binds to tubulin and prevents microtubule formation," *FASEB Journal*, vol. 21, no. 11, pp. 2787–2797, 2007.

[21] T. H. Davies and E. R. Sánchez, "FKBP52," *International Journal of Biochemistry and Cell Biology*, vol. 37, no. 1, pp. 42–47, 2005.

[22] K. P. Lu, Y. Liou, and X. Z. Zhou, "Pinning down proline-directed phosphorylation signaling," *Trends in Cell Biology*, vol. 12, no. 4, pp. 164–172, 2002.

[23] K. P. Lu and X. Z. Zhou, "The prolyl isomerase PIN1: a pivotal new twist in phosphorylation signalling and disease," *Nature Reviews Molecular Cell Biology*, vol. 8, no. 11, pp. 904–916, 2007.

[24] B. Ruan, K. Pong, F. Jow et al., "Binding of rapamycin analogs to calcium channels and FKBP52 contributes to their neuroprotective activities," *Proceedings of the National Academy of Sciences of the United States of America*, vol. 105, no. 1, pp. 33–38, 2008.

[25] J. Liu, J. D. Farmer Jr., W. S. Lane, J. Friedman, I. Weissman, and S. L. Schreiber, "Calcineurin is a common target of cyclophilin-cyclosporin A and FKBP-FK506 complexes," *Cell*, vol. 66, no. 4, pp. 807–815, 1991.

[26] C. R. Kissinǵer, H. E. Parge, D. R. Knighton et al., "Crystal structures of human calcineurin and the human FKBP12-FK506-calcineurin complex," *Nature*, vol. 378, no. 6557, pp. 641–644, 1995.

[27] L. C. Reese, F. Laezza, R. Woltjer, and G. Taglialatela, "Dysregulated phosphorylation of Ca2+/calmodulin-dependent protein kinase II-α in the hippocampus of subjects with mild cognitive impairment and Alzheimer's disease," *Journal of Neurochemistry*, vol. 119, no. 4, pp. 791–804, 2011.

[28] T. H. Davies, Y. Ning, and E. R. Sánchez, "Differential control of glucocorticoid receptor hormone-binding function by tetratricopeptide repeat (TPR) proteins and the immunosuppressive ligand FK506," *Biochemistry*, vol. 44, no. 6, pp. 2030–2038, 2005.

[29] M. D. Galigniana, A. G. Erlejman, M. Monte, C. Gomez-Sanchez, and G. Piwien-Pilipuk, "The hsp90-FKBP52 complex links the mineralocorticoid receptor to motor proteins and persists bound to the receptor in early nuclear events," *Molecular and Cellular Biology*, vol. 30, no. 5, pp. 1285–1298, 2010.

[30] D. L. Cioffi, T. R. Hubler, and J. G. Scammell, "Organization and function of the FKBP52 and FKBP51 genes," *Current Opinion in Pharmacology*, vol. 11, no. 4, pp. 308–313, 2011.

[31] H. R. Quintá and M. D. Galigniana, "The neuroregenerative mechanism mediated by the Hsp90-binding immunophilin FKBP52 resembles the early steps of neuronal differentiation," *British Journal of Pharmacology*, vol. 166, no. 2, pp. 637–649, 2012.

[32] H. R. Quintá, D. Maschi, C. Gomez-Sanchez, G. Piwien-Pilipuk, and M. D. Galigniana, "Subcellular rearrangement of hsp90-binding immunophilins accompanies neuronal differentiation and neurite outgrowth," *Journal of Neurochemistry*, vol. 115, no. 3, pp. 716–734, 2010.

[33] A. Castañeda-Ovando, M. D. L. Pacheco-Hernández, M. E. Páez-Hernández, J. A. Rodríguez, and C. A. Galán-Vidal, "Chemical studies of anthocyanins: a review," *Food Chemistry*, vol. 113, no. 4, pp. 859–871, 2009.

[34] F. C. Stintzing and R. Carle, "Functional properties of anthocyanins and betalains in plants, food, and in human nutrition," *Trends in Food Science and Technology*, vol. 15, no. 1, pp. 19–38, 2004.

[35] J. M. Kong, L. S. Chia, N. K. Goh, T. F. Chia, and R. Brouillard, "Analysis and biological activities of anthocyanins," *Phytochemistry*, vol. 64, no. 5, pp. 923–933, 2003.

[36] S. S. Percival, "Grape consumption supports immunity in animals and humans," *Journal of Nutrition*, vol. 139, supplement 9, pp. 1801S–1805S, 2009.

[37] C. Zhao, M. M. Giusti, M. Malik, M. P. Moyer, and B. A. Magnuson, "Effects of commercial anthocyanin-rich on colonic cancer and nontumorigenic colonic cell growth," *Journal of Agricultural and Food Chemistry*, vol. 52, no. 20, pp. 6122–6128, 2004.

[38] J. W. Hyun and H. S. Chung, "Cyanidin and malvidin from Oryza sativa cv. heugjinjubyeo mediate cytotoxicity against human monocytic leukemia cells by arrest of G 2/M phase and induction of apoptosis," *Journal of Agricultural and Food Chemistry*, vol. 52, no. 8, pp. 2213–2217, 2004.

[39] H. Jin, Q. Leng, and C. Li, "Dietary flavonoid for preventing colorectal neoplasms," *Cochrane Database of Systematic Reviews*, vol. 8, Article ID CD009350, 2012.

[40] H. P. Huang, Y. C. Chang, C. H. Wu, C. N. Hung, and C. Wang, "Anthocyanin-rich Mulberry extract inhibit the gastric cancer cell growth in vitro and xenograft mice by inducing signals of p38/p53 and c-jun," *Food Chemistry*, vol. 129, no. 4, pp. 1703–1709, 2011.

[41] T. Tsuda, F. Horio, and T. Osawa, "Cyanidin 3-O-β-D-glucoside suppresses nitric oxide production during a zymosan treatment in rats," *Journal of Nutritional Science and Vitaminology*, vol. 48, no. 4, pp. 305–310, 2002.

[42] X. Xia, W. Ling, J. Ma et al., "An anthocyanin-rich extract from black rice enhances atherosclerotic plaque stabilization in apolipoprotein E-deficient mice," *Journal of Nutrition*, vol. 136, no. 8, pp. 2220–2225, 2006.

[43] A. Jennings, A. A. Welch, S. J. Fairweather-Tait et al., "Higher anthocyanin intake is associated with lower arterial stiffness and central blood pressure in women," *The American Journal of Clinical Nutrition*, vol. 96, no. 4, pp. 781–788, 2012.

[44] S. S. Hassellund, A. Flaa, S. E. Kjeldsen et al., "Effects of anthocyanins on cardiovascular risk factors and inflammation in pre-hypertensive men: a double-blind randomized placebo-controlled crossover study," *Journal of Human Hypertension*, vol. 27, no. 2, pp. 100–106, 2013.

[45] D. Ghosh and T. Konishi, "Anthocyanins and anthocyanin-rich extracts: role in diabetes and eye function," *Asia Pacific Journal of Clinical Nutrition*, vol. 16, no. 2, pp. 200–208, 2007.

[46] M. K. Kang, J. Li, J. L. Kim et al., "Purple corn anthocyanins inhibit diabetes-associated glomerular monocyte activation and macrophage infiltration," *American Journal of Physiology Renal Physiology*, vol. 303, no. 7, pp. F1060–F1069, 2012.

[47] S. H. Nam, S. P. Choi, M. Y. Kang, H. J. Koh, N. Kozukue, and M. Friedman, "Antioxidative activities of bran extracts from twenty one pigmented rice cultivars," *Food Chemistry*, vol. 94, no. 4, pp. 613–620, 2006.

[48] M. Philpott, K. S. Gould, C. Lim, and L. R. Ferguson, "In situ and in vitro antioxidant activity of sweetpotato anthocyanins," *Journal of Agricultural and Food Chemistry*, vol. 52, no. 6, pp. 1511–1513, 2004.

[49] Y. Wang, X. Chen, Y. Zhang, and X. Chen, "Antioxidant activities and major anthocyanins of myrobalan plum (Prunus cerasifera Ehrh.)," *Journal of Food Science*, vol. 77, no. 4, pp. C388–C393, 2012.

[50] S. J. Chen, J. G. Chung, Y. C. Chung, and S. T. Chou, "In vitro antioxidant and antiproliferative activity of the stem extracts from graptopetalum paraguayense," *American Journal of Chinese Medicine*, vol. 36, no. 2, pp. 369–383, 2008.

[51] Y. L. Ho, S. S. Huang, J. S. Deng, Y. Lin, Y. Chang, and G. Huang, "In vitro antioxidant properties and total phenolic contents of wetland medicinal plants in Taiwan," *Botanical Studies*, vol. 53, no. 1, pp. 55–66, 2012.

[52] M. Miyazawa, T. Oshima, K. Koshio, Y. Itsuzaki, and J. Anzai, "Tyrosinase inhibitor from black rice bran," *Journal of Agricultural and Food Chemistry*, vol. 51, no. 24, pp. 6953–6956, 2003.

[53] J. Yamakoshi, F. Otsuka, A. Sano et al., "Lightening effect on ultraviolet-induced pigmentation of Guinea pig skin by oral administration of a proanthocyanidin-rich extract from grape seeds," *Pigment Cell Research*, vol. 16, no. 6, pp. 629–638, 2003.

[54] C. Gómez-Cordovés, B. Bartolomé, W. Vieira, and V. M. Virador, "Effects of wine phenolics and sorghum tannins on tyrosinase activity and growth of melanoma cells," *Journal of Agricultural and Food Chemistry*, vol. 49, no. 3, pp. 1620–1624, 2001.

[55] T. Hanamura, E. Uchida, and H. Aoki, "Skin-lightening effect of a polyphenol extract from acerola (Malpighia emarginata DC.) fruit on UV-induced pigmentation," *Bioscience, Biotechnology and Biochemistry*, vol. 72, no. 12, pp. 3211–3218, 2008.

[56] M. Dell'Agli, G. V. Galli, U. Vrhovsek, F. Mattivi, and E. Bosisio, "In vitro inhibition of human cGMP-specific phosphodiesterase-5 by polyphenols from red grapes," *Journal of Agricultural and Food Chemistry*, vol. 53, no. 6, pp. 1960–1965, 2005.

[57] M. Hattori, E. Sugino, K. Minoura et al., "Different inhibitory response of cyanidin and methylene blue for filament formation of tau microtubule-binding domain," *Biochemical and Biophysical Research Communications*, vol. 374, no. 1, pp. 158–163, 2008.

[58] P. H. Shih, Y. C. Chan, J. W. Liao, M. F. Wang, and G. C. Yen, "Antioxidant and cognitive promotion effects of anthocyanin-rich mulberry (Morus atropurpurea L.) on senescence-accelerated mice and prevention of Alzheimer's disease," *Journal of Nutritional Biochemistry*, vol. 21, no. 7, pp. 598–605, 2010.

[59] Y. Zuo, C. Peng, Y. Liang et al., "Black rice extract extends the lifespan of fruit flies," *Food & Function*, vol. 3, no. 12, pp. 1271–1279, 2012.

[60] P. H. Shih, C. H. Wu, C. T. Yeh, and G. C. Yen, "Protective effects of anthocyanins against amyloid β-peptide-induced damage in neuro-2A Cells," *Journal of Agricultural and Food Chemistry*, vol. 59, no. 5, pp. 1683–1689, 2011.

[61] H. J. Huang, H. W. Yu, C. Y. Chen et al., "Current developments of computer-aided drug design," *Journal of the Taiwan Institute of Chemical Engineers*, vol. 41, no. 6, pp. 623–635, 2010.

[62] C. Y. C. Chen, "A novel integrated framework and improved methodology of computer-aided drug design," *Current Topics in Medicinal Chemistry*, vol. 13, no. 9, pp. 965–988, 2013.

[63] C. Y. Chen, "A novel integrated framework and improved methodology of computer-aided drug design," *Current Topics in Medicinal Chemistry*, vol. 13, no. 9, pp. 965–988, 2013.

[64] Y. Yoshiyama, M. Higuchi, B. Zhang et al., "Synapse loss and microglial activation precede tangles in a P301S tauopathy mouse model," *Neuron*, vol. 53, no. 3, pp. 337–351, 2007.

[65] K. T. Dineley, R. Kayed, V. Neugebauer et al., "Amyloid-β oligomers impair fear conditioned memory in a calcineurin-dependent fashion in mice," *Journal of Neuroscience Research*, vol. 88, no. 13, pp. 2923–2932, 2010.

[66] T. L. Spires-Jones, K. Kay, R. Matsouka, A. Rozkalne, R. A. Betensky, and B. T. Hyman, "Calcineurin inhibition with systemic FK506 treatment increases dendritic branching and dendritic spine density in healthy adult mouse brain," *Neuroscience Letters*, vol. 487, no. 3, pp. 260–263, 2011.

[67] A. Rozkalne, B. T. Hyman, and T. L. Spires-Jones, "Calcineurin inhibition with FK506 ameliorates dendritic spine density deficits in plaque-bearing Alzheimer model mice," *Neurobiology of Disease*, vol. 41, no. 3, pp. 650–654, 2011.

[68] J. Q. Trojanowski, K. Duff, H. Fillit et al., "New directions for frontotemporal dementia drug discovery," *Alzheimer's and Dementia*, vol. 4, no. 2, pp. 89–93, 2008.

[69] T. E. Starzl, J. Fung, R. Venkataramman, S. Todo, A. J. Demetris, and A. Jain, "FK 506 for liver, kidney, and pancreas transplantation," *The Lancet*, vol. 2, no. 8670, pp. 1000–1004, 1989.

[70] R. Shapiro, J. J. Fung, A. B. Jain, P. Parks, S. Todo, and T. E. Starzl, "The side effects of FK 506 in humans," *Transplantation Proceedings*, vol. 22, no. 1, pp. 35–36, 1990.

[71] N. Mohebbi, M. Mihailova, and C. A. Wagner, "The calcineurin inhibitor FK506 (tacrolimus) is associated with transient metabolic acidosis and altered expression of renal acid-base transport proteins," *American Journal of Physiology-Renal Physiology*, vol. 297, no. 2, pp. F499–F509, 2009.

[72] E. M. Haddad, V. C. McAlister, E. Renouf, R. Malthaner, M. S. Kjaer, and L. L. Gluud, "Cyclosporin versus tacrolimus for liver transplanted patients," *Cochrane Database of Systematic Reviews*, no. 4, Article ID CD005161, 2006.

[73] T. Ochiai, M. Nagata, K. Nakajima et al., "Studies of the effects of FK506 on renal allografting in the beagle dog," *Transplantation*, vol. 44, no. 6, pp. 729–733, 1987.

[74] W.-L. Liao and F.-J. Tsai, "Personalized medicine: a paradigm shift in healthcare," *BioMedicine*, vol. 3, no. 2, pp. 66–72, 2013.

[75] F.-J. Tsai, "Biomedicine brings the future nearer," *Biomedicine*, 2011.

[76] F.-J. Tsai, "Rare diseases: a mysterious puzzle," *BioMedicine*, vol. 3, no. 2, p. 65, 2013.

[77] C.-H. Wang, W.-D. Lin, and F.-J. Tsai, "Craniofacial dysmorphism, what is your diagnosis?" *BioMedicine*, vol. 2, no. 2, pp. 49–50, 2012.

[78] C. Y. Chen, "TCM Database@Taiwan: the world's largest traditional Chinese medicine database for drug screening In Silico," *PLoS ONE*, vol. 6, no. 1, Article ID e15939, 2011.

[79] K. C. Chen and C. Y. C. Chen, "Stroke prevention by traditional Chinese medicine? A genetic algorithm, support vector machine and molecular dynamics approach," *Soft Matter*, vol. 7, no. 8, pp. 4001–4008, 2011.

[80] K. C. Chen, M. F. Sun, S. C. Yang et al., "Investigation into potent inflammation inhibitors from traditional Chinese medicine," *Chemical Biology and Drug Design*, vol. 78, no. 4, pp. 679–688, 2011.

[81] W. I. Tou, S. S. Chang, C. C. Lee, and C. Y. Chen, "Drug design for neuropathic pain regulation from traditional Chinese medicine," *Scientific Reports*, vol. 3, p. 844, 2013.

[82] S. C. Yang, S. S. Chang, H. Chen, and C. Y. Chen, "Identification of potent EGFR inhibitors from TCM Database@Taiwan," *PLoS Computational Biology*, vol. 7, no. 10, Article ID e1002189, 2011.

[83] S. C. Yang, S. S. Chang, and C. Y. Chen, "Identifying HER2 inhibitors from natural products database," *PLoS ONE*, vol. 6, no. 12, Article ID e28793, 2011.

[84] S. S. Chang, H. J. Huang, and C. Y. C. Chen, "Two birds with one stone? Possible dual-targeting H1N1 inhibitors from traditional Chinese medicine," *PLoS Computational Biology*, vol. 7, no. 12, Article ID e1002315, 2011.

[85] T. T. Chang, M. F. Sun, H. Y. Chen et al., "Screening from the world's largest TCM database against H1N1 virus," *Journal of Biomolecular Structure and Dynamics*, vol. 28, no. 5, pp. 773–786, 2011.

[86] T. Y. Tsai, K. W. Chang, and C. Y. Chen, "IScreen: World's first cloud-computing web server for virtual screening and de novo drug design based on TCM database@Taiwan," *Journal of Computer-Aided Molecular Design*, vol. 25, no. 6, pp. 525–531, 2011.

[87] B. Wu, P. Li, Y. Liu et al., "3D structure of human FK506-binding protein 52: implication for the assembly of the glucocorticoid receptor/Hsp90/immunophilin heterocomplex," *Proceedings of the National Academy of Sciences of the United States of America*, vol. 101, no. 22, pp. 8348–8353, 2004.

[88] Y. Wang, E. Bolton, S. Dracheva et al., "An overview of the PubChem BioAssay resource," *Nucleic Acids Research*, vol. 38, no. 1, Article ID gkp965, pp. D255–D266, 2009.

[89] W. I. Tou and C. Y. Chen, "May disordered protein cause serious drug side effect?" *Drug Discovery Today*, vol. 19, no. 4, pp. 367–372, 2014.

[90] C. Y. C. Chen and W. L. Tou, "How to design a drug for the disordered proteins," *Drug Discovery Today*, vol. 18, no. 19-20, pp. 910–915, 2013.

[91] C. M. Venkatachalam, X. Jiang, T. Oldfield, and M. Waldman, "LigandFit: a novel method for the shape-directed rapid docking of ligands to protein active sites," *Journal of Molecular Graphics and Modelling*, vol. 21, no. 4, pp. 289–307, 2003.

[92] R. A. Laskowski and M. B. Swindells, "LigPlot+: multiple ligand-protein interaction diagrams for drug discovery," *Journal of Chemical Information and Modeling*, vol. 51, no. 10, pp. 2778–2786, 2011.

[93] B. R. Brooks, C. L. Brooks III, A. D. Mackerell Jr. et al., "CHARMM: the biomolecular simulation program," *Journal of Computational Chemistry*, vol. 30, no. 10, pp. 1545–1614, 2009.

[94] R. Fletcher, *Optimization*, Academic Press, New York, NY, USA, 1969.

[95] R. Fletcher and C. M. Reeves, "Function minimization by conjugate gradients," *Computer Journal*, vol. 7, no. 2, pp. 149–154, 1964.

[96] J. H. Peters and B. L. de Groot, "Ubiquitin dynamics in complexes reveal molecular recognition mechanisms beyond induced fit and conformational selection," *PLOS Computational Biology*, vol. 8, no. 10, Article ID e1002704, 2012.

[97] P. Li, Y. Ding, B. Wu, C. Shu, B. Shen, and Z. Rao, "Structure of the N-terminal domain of human FKBP52," *Acta Crystallographica D: Biological Crystallography*, vol. 59, no. 1, pp. 16–22, 2003.

[98] D. L. Riggs, M. B. Cox, H. L. Tardif, M. Hessling, J. Buchner, and D. F. Smith, "Noncatalytic role of the FKBP52 peptidyl-prolyl isomerase domain in the regulation of steroid hormone signaling," *Molecular and Cellular Biology*, vol. 27, no. 24, pp. 8658–8669, 2007.

[99] C. R. Sinars, J. Cheung-Flynn, R. A. Rimerman, J. G. Scammell, D. F. Smith, and J. Clardy, "Structure of the large FK506-binding protein FKBP51, an Hsp90-binding protein and a component of steroid receptor complexes," *Proceedings of the National Academy of Sciences of the United States of America*, vol. 100, no. 3, pp. 868–873, 2003.